ADVANCES IN INORGANIC CHEMISTRY AND RADIOCHEMISTRY, VOL. 28

HOMOCYCLIC SELENIUM MOLECULES AND RELATED CATIONS

RALF STEUDEL and EVA-MARIA STRAUSS

Institut für Anorganische und Analytische Chemie, Technische Universität Berlin, Berlin, Federal Republic of Germany

I. General 135
II. Neutral Selenium Ring Molecules 136
A. Cyclopentaselenium, Se_5 136
B. Cyclohexaselenium, Se_6 137
C. Cycloheptaselenium, Se_7 142
D. Cyclooctaselenium, Se_8 144
E. Other Ring Molecules 150
F. Thermodynamic Properties of Selenium Allotropes 151
III. Homocyclic Selenium Cations 152
A. Mass Spectra of Selenium Vapors 154
B. Dications Se_n^{2+} in Solids and Solutions 155
C. Other Dications 160
IV. Selenium Iodide Cations, Se_nI^+ 161
V. Conclusions and Outlook 162
References 163

I. General

The heavier chalkogens are known for their tendency toward homonuclear catenation, which rivals that of phosphorus and silicon and is exceeded only by that of carbon. Especially sulfur forms a large number of rings S_n (n = 6, 7, ...) (*1*) and of chainlike compounds of type R—S_n—R (R = inorganic or organic group) (*2*), which have been extensively studied. In the case of selenium the number of known cyclic compounds with more than one Se—Se bond, that is, compounds with cumulated Se—Se bonds, was formerly quite small, and for a long time the Se_8 molecule was the only example. However, developments have shown that selenium is able to form rings Se_n of various sizes as well as cyclic, bicyclic, and cagelike dications Se_n^{2+}, and cyclic derivatives like

ISBN 0-12-023628-1

TABLE I

PRESENTLY KNOWN HOMOCYCLIC SELENIUM COMPOUNDS

Neutral rings		Monocations	Dications	Ring derivatives
As pure materials:	Se_6, Se_8	Se_n^+ (n = 5 ... 10)	Se_n^{2+}	$[Se_6I][AsF_6]$
In solution:	Se_n (n = 6–8)	(in the vapor	(n = 4, 8, or 10)	
In the gas phase:	Se_n (n = 5–10)	phase only)		

Se_6I^+, as does sulfur. In addition, a number of presumably cyclic monocations Se_n^+ have been studied in the vapor phase.

The presently known homocyclic selenium compounds are summarized in Table I. All these compounds are interesting owing to their chemical simplicity—the allotropes of an element and its binary derivatives should interest every chemist—and their bond properties. Furthermore, homocyclic selenium species are related to the much studied and still poorly understood semiconducting amorphous selenium, which may be a mixture of chain- and ringlike molecules similar to liquid or amorphous (polymeric) sulfur. In this connection, the small rings Se_6, Se_7, and Se_8 can serve as model species to study the chemical transformations of amorphous selenium on heating or on irradiation, as well as the changes in its chemical and physical properties on doping or because of the presence of impurities. Selenium–selenium bonds are of lower bond energy and consequently of higher reactivity than comparable sulfur–sulfur bonds. The preparation and characterization of compounds containing cumulated Se–Se bonds therefore require more sophisticated preparative and analytical methods. The later results in this field are reviewed in this article; for earlier reviews, see refs. (*3–7*).

II. Neutral Selenium Ring Molecules

Neutral selenium rings Se_n have been studied in the vapor phase by mass spectroscopy, in solution by high-pressure liquid chromatography, and in the solid state by Raman spectroscopy and X-ray crystallography.

A. CYCLOPENTASELENIUM, Se_5

The five-membered ring Se_5 is one of the major components of selenium vapor. However, despite several extensive investigations, there

is still no agreement between different authors regarding the quantitative molecular composition of the saturated vapor above metallic ("gray") or liquid selenium (mp 221°C, 494 K). The Se_5 concentration in the vapor has been derived from vapor-pressure measurements as well as from EI mass-spectrometric studies, using 10-eV electrons whose energy is sufficient for ionization but not for fragmentation plus ionization of molecules larger than Se_5. Near 470 K, Se_5 concentrations of between 15 and 50% and at 1000 K between 20 and 55% have been found (*8–11*) (see also Fig. 1). For the vapor leaving the surface of metallic selenium ("freely subliming selenium") a concentration of $\leq$29% Se_5 has been determined at 448 K, using 40-eV electrons (*12*). The thermodynamic data for Se_5 (see Section II,F) indicate that the molecule is cyclic rather than a chain, but the accurate structure is unknown since pure Se_5, like pure S_5, has never been prepared. There is also no evidence for the presence of Se_5 in solutions.

B. Cyclohexaselenium, Se_6

Cyclohexaselenium is the main component of the vapor above freely subliming metallic selenium, accounting for as much as 58% of the vapor at 448 K (*12, 13*). In the saturated vapor above metallic or liquid selenium, Se_6 is also one of the main species at temperatures up to about 800–850 K, but there is no close agreement between the quantitative data published by different authors (*8–11*) (see also Fig. 1). By angular distribution mass spectrometry, a concentration of 40% Se_6 has been determined at 463 K (*11*).

By high-pressure liquid chromatography, using a UV absorbance detector, cyclohexaselenium has been detected in various selenium solutions in equilibrium with Se_7 and Se_8 (see also Section II,D) (*14*). Cyclohexaselenium is also formed by thermal decomposition of Se_7 in inert organic solvents like CS_2 according to the equation

$$2Se_7 \longrightarrow Se_6 + Se_8$$

(see Section II,C) (*15*).

1. Preparation

Crystalline Se_6 has been prepared. The synthesis consists of some kind of recrystallization of red amorphous selenium, prepared from highly purified selenium, which is extracted with carbon disulfide. By a special crystallization method, two types of single crystals have been

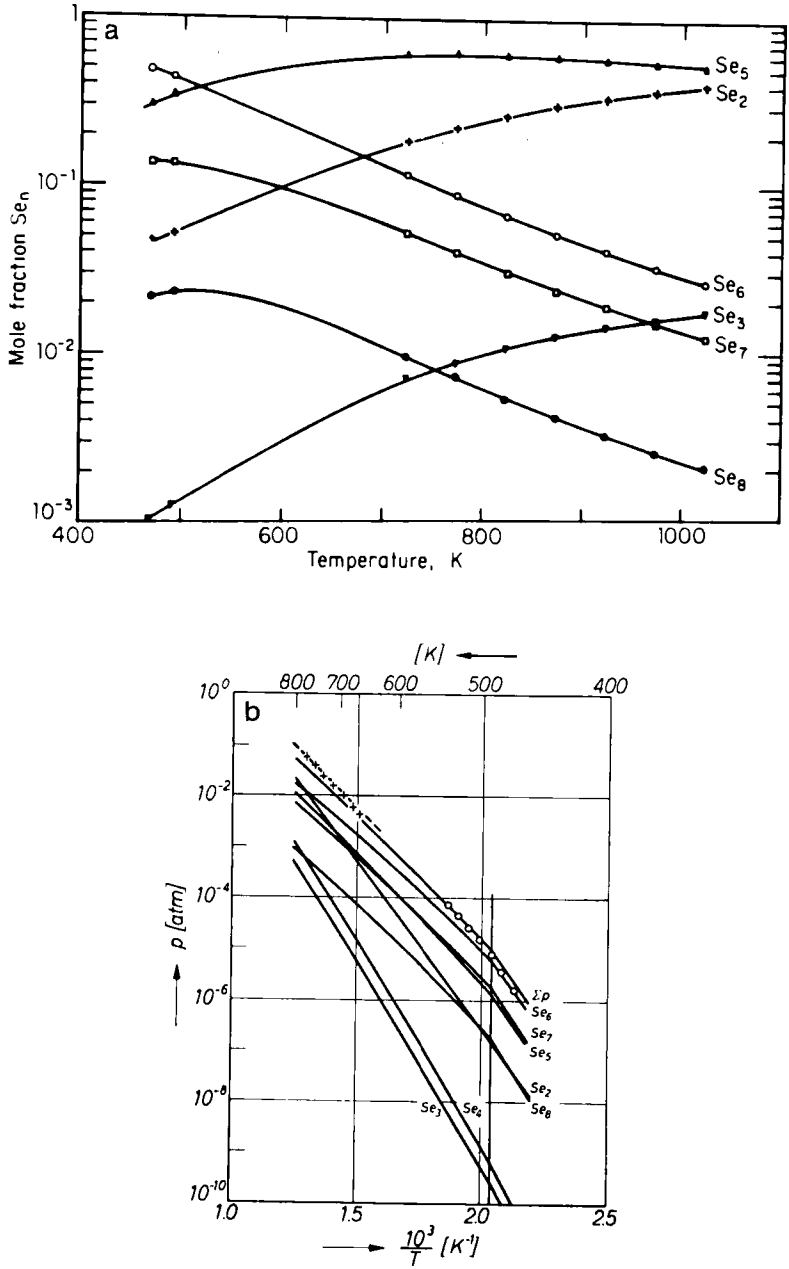

FIG. 1. Molecular composition of saturated selenium vapor: (a) according to Berkowitz *et al.* (*8*) [cited in (*4a*)]; (b) according to Keller *et al.* (*9*) (1 atm = 1.013 bar).

obtained from the solution and the needlelike cyclohexaselenium was separated under a microscope from the well-known α-monoclinic Se_8 (*16*), and characterized by X-ray crystallography, vibrational spectroscopy, and differential scanning calorimetry (DSC) (*16–19*).

The only known *chemical* synthesis of Se_6 is based on the reactions

$$Se_2Cl_2 + 2KI \xrightarrow[20°C]{CS_2} Se_2I_2 + 2KCl$$

$$nSe_2I_2 \xrightarrow{20°C} Se_{2n} + nI_2 \ (n = 6 \text{ or } 8)$$

which are analogous to the synthesis of S_6 from S_2Cl_2 (*20*). A crystalline mixture of Se_6 and Se_8 is obtained in which the two components can be detected by low-temperature Raman spectroscopy (*15*).

2. *Molecular Structure and Bonding*

Cyclohexaselenium crystallizes in the rhombohedral space group $R\bar{3}$ and therefore represents a second form of "trigonal selenium" besides the well-known gray or "metallic" or "hexagonal" or "trigonal" selenium (space group $P3_121$), which is polymeric and represents the thermodynamically stable allotrope at 25°C/1.013 bar. In order to avoid misunderstandings, in this review, cyclohexaselenium will simply be termed Se_6 or rhombohedral selenium, and gray selenium (Se_∞) will be called trigonal or metallic selenium. Other presumably polymeric forms of selenium are the "glassy" or "vitreous" selenium, obtained by quenching of liquid selenium, and the two forms of "red amorphous" selenium (*5*), obtained either by quenching of selenium vapor in liquid nitrogen (*21*) or by chemical reduction of water-soluble selenium compounds (*22*) (e.g., SeO_2) with SO_2 or hydrazine. In this article, the latter two forms will be termed as "red amorphous Se(vap)" and "red amorphous Se(redn)." Since red amorphous Se(redn) turns irreversibly black at 30°C (*19*) the "black amorphous Se" obtained in this way is sometimes regarded as another form of elemental selenium.

According to a complete X-ray diffraction analysis, Se_6 consists of ring molecules with the molecular symmetry of D_{3d}; the crystal and molecular parameters are listed in Table II (*17*) and the crystal structure is shown in Fig. 2. Refinement by the least squares method resulted in the following atomic parameters of the single atom in the asymmetric unit: $x = 0.1602 \pm 0.00048$, $y = 0.20227 \pm 0.00047$, $z = 0.12045 \pm 0.00120$; calculated density, 4.71 g/cm^3. An earlier investigation of selenium vapor by electron diffraction led to an internuclear distance of 234 ± 1 pm and an average bond angle of 102 ± 0.5° for the chairlike cyclic Se_6 molecule (*23*).

TABLE II

CRYSTAL AND MOLECULAR PARAMETERS OF Se_6, α-, β-, AND γ-Se_8, AND METALLIC SELENIUM (Se_∞)

	Se_6 [17][a]	α-Se_8 [31][a]	β-Se_8 [28][a]	γ-Se_8 [29][a]	Se_∞ [32, 33][a]
Space group	$R\bar{3}$	$P2_1/n$	$P2_1/a$	$P2_1/c$	$P3_121$
Crystal data (20°C)	a = 1136.2(1)	a = 905.4 ± 0.3	a = 1285	a = 1501.8(1)	a = 436.6
(a,b,c in pm)	c = 442.9(8)	b = 908.3 ± 0.5	b = 807	b = 1471.3(1)	c = 495.8
		c = 1160.1 ± 0.6	c = 931	c = 878.9(1)	
		β = 90.81 ± 0.05°	β = 93.75	β = 93.61(1)	
Z (number of molecules in unit cell)	3	4	4	8	3 (atoms)
Calculated density (g/cm^3)	4.71	4.400	4.352	4.33	4.807
Site symmetry of the molecules in the crystal structure	D_{3d}	C_1	C_1	C_1	—
Average Se—Se bond length (pm)	235.6 ± 0.9	233.6(6)	234 ± 1.4	233.4 ± 0.5	237.4 ± 0.5
Average Se—Se—Se bond angle	101.1 ± 0.3°	105.7(1.6)°	105.7 ± 0.8	105.8 ± 1.4	103.1 ± 0.2
Average torsional angle	76.2 ± 0.4°	101.3°	101.4°	101 ± 2°	100.7 ± 0.1°
Shortest intermolecular distance (pm)	341.4	347.6	340	334.6	343.6

[a] Numbers in brackets indicate standard deviations.

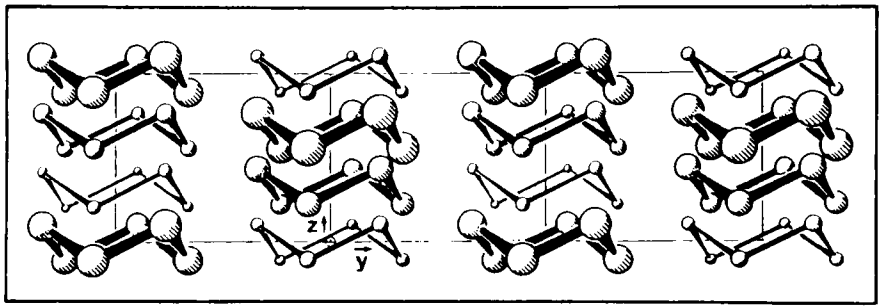

FIG. 2. Molecular and crystal structure of cyclohexaselenium, Se_6.

3. *Molecular Spectra*

Infrared and Raman spectra of Se_6 have been measured, and the observed wave numbers have been assigned to the eight fundamental vibrations by comparison with the wave numbers calculated from force constants taken from Se_8 and using a modified Urey–Bradley force field. The spectra of S_6 and Se_6 are completely analogous (see Table III). The four *g* vibrations are Raman active, the three a_{2u} and e_u vibrations are active in the infrared while the a_{1u} mode cannot be observed directly.

By adjusting the calculated to the observed wave numbers, the following five Urey–Bradley force constants have been obtained for Se_6 (in N/cm): $K = 1.188$ (bond stretching), $H = 0.102$ (bond-angle bending), $F = 0.082$ (next nearest atom repulsion), $Y = 0.242$ (torsion), and $P = 0.207$ (bond–bond interaction) (*18, 19*).

4. *Chemical Properties and Reactions*

Since pure Se_6 has so far been prepared only in minute amounts, its chemical properties have hardly been explored. Differential scanning

TABLE III

OBSERVED AND CALCULATED WAVE NUMBERS[a] OF THE EIGHT FUNDAMENTAL MODES OF CYCLOHEXASELENIUM, Se_6 (*19*)

	ν_1	ν_2	ν_3	ν_4	ν_5	ν_6	ν_7	ν_8
Symmetry	a_{1g}	a_{1g}	a_{1u}	a_{2u}	e_g	e_g	e_u	e_u
Observed	247	129	—	151	221	102	253	103
Calculated	264	126	216	154	236	102	257	83

[a] In cm^{-1}.

TABLE IV

APPEARANCE POTENTIALS OF SELENIUM MOLECULAR IONS[a]

	Reference (*8*)	Reference (*12*)
Se_5^+	8.6 ± 0.2	9.2 ± 0.2
Se_6^+	8.9 ± 0.2	9.08 ± 0.05
Se_7^+	8.4 ± 0.2	8.87 ± 0.05
Se_8^+	8.6 ± 0.2	8.97 ± 0.05

[a] In eV.

calorimetry measurements on Se_6 crystals from 373 K up to the melting point of metallic selenium (494 K) have been carried out. They show a small endothermic peak near 393 K and an exothermic peak at 408 K, which have been attributed in terms of melting and recrystallization, respectively, to the polymeric metallic phase (*17*).

C. CYCLOHEPTASELENIUM, Se_7

The seven-membered ring Se_7 has been established as part of the vapor above freely subliming selenium in an amount of 11.4% at 448 K (*12, 13*). The equilibrium concentration in the saturated vapor above metallic or liquid selenium is of the same order of magnitude but decreases rapidly with temperature (see Fig. 1) (*8–11*).

Since the ionization potential of Se_7 is lower than that of both Se_6 and Se_8 (see Table IV), as has also been observed in the case of the corresponding sulfur rings, the structure of Se_7 should be analogous to that of S_7, which forms a chairlike molecule of C_s symmetry:

The torsional angle of 0° at the unique bond results in a strong repulsion of lone electron pairs, leading to a relatively low ionization energy (*24*).

Cycloheptaselenium been detected in various solutions by HPLC, using a column with octadecylsilane as a stationary phase in connection with a UV absorbance detector. The retention time of the Se_7 molecule is between those of Se_6 and Se_8, in complete analogy to the

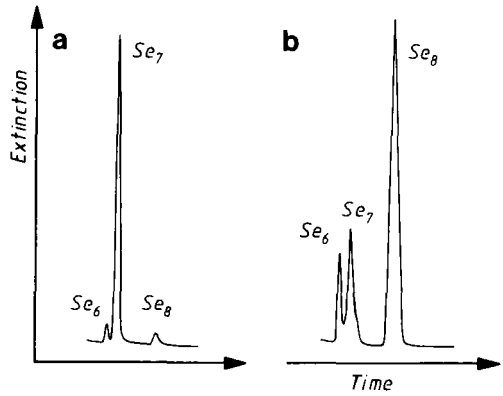

FIG. 3. Chromatogram (HPLC) of a solution of Se_7 in CS_2 at 25°C (*15*); (a) freshly prepared; (b) after 4 hr at 25°C in the dark.

behavior of the corresponding sulfur rings (*1, 14*). Cycloheptaselenium-containing solutions are obtained by dissolution of Se_8 or of red amorphous Se(redn) since the following equilibrium is established within several minutes at 25°C (*14*):

$$Se_8 \rightleftharpoons 8/7\ Se_7 \rightleftharpoons 4/3\ Se_6 \tag{1}$$

However, only small relative concentrations of Se_7 (with regard to Se_8) are obtained in this way. Almost pure Se_7 solutions can be prepared from titanocenepentaselenide and dichlorodiselane (Se_2Cl_2) according to the following equation (*15*):

$$(C_5H_5)_2TiSe_5 + Se_2Cl_2 \longrightarrow Se_7 + (C_5H_5)_2TiCl_2 \tag{2}$$

The chromatogram of this solution is shown in Fig. 3a; after 4 hr at 25°C, equilibrium [Eq. (1)] is established, and the chromatogram shown in Fig. 3b is obtained (*15*). The interconversion of Se_7 to Se_8 obviously begins with the reaction

$$2Se_7 \longrightarrow Se_6 + Se_8 \tag{3}$$

which is followed by the decomposition of the Se_6 by a still unknown reaction path (presumably via intermediate formation of larger rings). The mechanism of the reaction shown in Eq. (3) very likely involves the formation of a transient intermediate with a four-coordinated selenium atom, as has also been proposed in the case of sulfur rings (*1*):

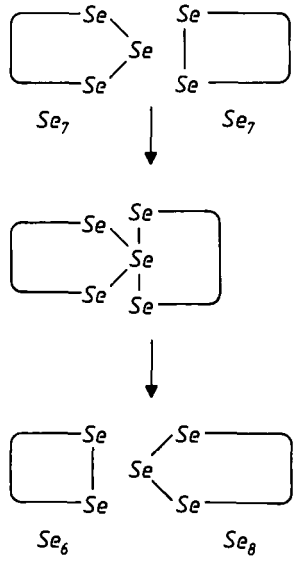

Dark-red crystals of another form of selenium have been grown from a CS_2 solution. X-ray rotating crystal and Weisenberg methods showed the material to be orthorhombic (or nearly so) with the lattice constants $a = 2632$, $b = 688$, and $c = 434$ pm, resulting in a unit-cell volume of 7.86×10^{-22} cm^3, which leads to a cell content of 28 atoms (observed density, 4.6 g/cm^3) (*25*). Thus the material may consist of Se_7 ring molecules.

D. Cyclooctaselenium, Se_8

1. Preparation

The crown-shaped molecule Se_8 has long been known to crystallize in two monoclinic lattices termed α- and β-Se_8, respectively (see Table II). Crystals of various sizes have been obtained from CS_2 solutions prepared by dissolution of either red amorphous Se (*22*) or of vitreous selenium in CS_2 and subsequent cooling or evaporation of the solvent (*3a,b, 4a, 5*). Red amorphous Se is readily soluble in CS_2, but since both vitreous and red amorphous Se do not contain more than small amounts of Se_8, the dissolution must be accompanied by a chemical interconversion. It has, however, been reported (*26*) that the dissolution of red amorphous Se in CS_2 requires illumination with photons of energies in excess of 2.3 eV, ambient room light levels being sufficient.

In the dark, the surface attack of CS_2 is said to leave a rubbery insoluble fraction similar to polymeric sulfur.

α- and β-Cyclooctaselenium form crystals of different shapes and with different interfacial angles and consequently can be separated under a microscope (*3b*). Slow evaporation of a saturated solution in CS_2 yields α-monoclinic Se_8, while on rapid evaporation α- and β-monoclinic Se_8 are formed (*27, 28*). Since the β form dissolves in a carbon disulfide solution saturated with the α form, the latter seems to be the more stable of the two (*29*). This observation is in agreement with the densities, which decrease in the order α-Se_8 > β-Se_8 > γ-Se_8 (see Table II). Large single crystals of α-monoclinic Se_8 have been grown from a solution in methylene iodide (*30*).

A third monoclinic allotrope, γ-Se_8, has been prepared from a solution of dipiperidinotetraselane in carbon disulfide (*29*):

$$Se_4(NC_5H_{10})_2 + 2CS_2 \longrightarrow 3/8\ Se_8 + Se(S_2CNC_5H_{10})_2$$

γ-Cyclooctaselenium forms long prisms with eight molecules in the unit cell (see Table II) and is quite stable at 25°C (*29*).

An investigation has shown that dissolution of crystalline Se_8 or extraction of glassy or red amorphous selenium (the latter prepared from aqueous SeO_2 by reduction) by different organic solvents yields solutions containing Se_6, Se_7, and Se_8 in equilibrium. Through high-pressure liquid chromatography on reversed bonded phases, the three rings Se_n have been separated and detected by their UV absorption at 254 nm. In contrast to selenium vapor, Se_8 is the main component (*14*). The total solubility of Se in CS_2 at 25°C amounts to 0.05% by weight or 0.008 mol (Se) per liter (*34, 35*). These results have led to the conclusion that Se_6, Se_7, and Se_8 undergo a rapid interconversion in solution at 25°C, leading to an equilibrium (*14*). The equilibrium vapor above metallic or liquid selenium contains only 1–2% Se_8 at temperatures of between 440 and 720 K (*8–12*).

The spontaneous but slow crystallization of monoclonic selenium (Se_8) from red amorphous Se, prepared by quenching of selenium vapor (1000°C) in liquid nitrogen, depends on the storage temperature of the samples. Below 303 K, red amorphous Se(vap) is completely transformed into the monoclinic phase, whereas above 303 K transformation into the metallic phase takes place. (The relative Se_8 content of the material can be determined by DSC.) In contrast, chemically prepared red amorphous Se(redn) is transformed only into the metallic phase, even below 303 K (*21*).

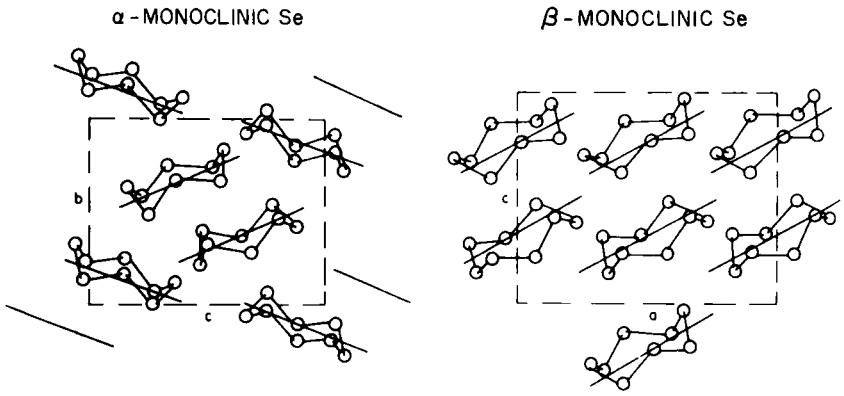

FIG. 4. Molecular and crystal structures of monoclinic α-Se_8 and β-Se_8.

2. *Molecular Structure and Bonding*

The crystal and molecular structure data of the three Se_8 forms listed in Table II have been determined by X-ray diffraction (*27–29, 31*). α-, β-, and γ-cyclooctaselenium crystallize in the same space group but differ in the packing of the molecules (see Fig. 4). The average bond distances, bond angles, and torsional angles of the Se_8 molecules are identical within the limits of the standard deviation. The torsional angle of 101° is close to the value of 99° observed in the case of S_8 (*36*) and obviously corresponds to the minimum of the torsional potential energy function. The shortest intermolecular distance has been observed in the case of γ-Se_8: the value of 334.6 pm is even smaller than the shortest intermolecular contact in orthorhombic cyclooctasulfur, S_8 [337 pm (*33*)].

3. *Molecular Spectra*

Raman and infrared spectra of α-monoclinic selenium have been reported (*3c,d, 4b, 14, 37*); the low-temperature Raman spectrum is shown in Fig. 5. It differs sufficiently from that of Se_6 for both compounds to be detected in this way in mixtures with each other (*15*). The observed wave numbers have been assigned to the 11 fundamental modes of the Se_8 molecule, assuming D_{4d} symmetry (see Table V). The b_2 and e_1 modes are infrared active, and the a_1, e_2, and e_3 vibrations are Raman active. The wave number of the inactive b_1 fundamental has been estimated from the second-order Raman spectrum.

Using an extended Urey–Bradley force field with six force constants,

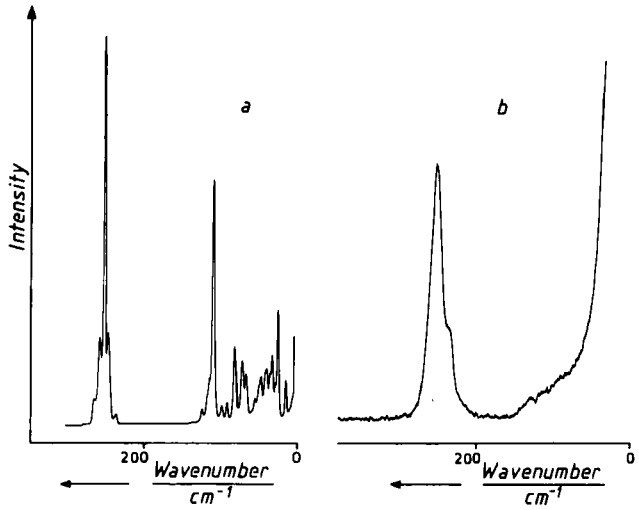

FIG. 5. Low-temperature Raman spectra (−105 ± 5°C) of monoclinic α-Se_8 (a) and of red amorphous selenium prepared by reduction of SeO_2 (b) (*14*).

a very good agreement between the observed and calculated wave numbers has been achieved. These force constants have the following values (in N/cm) (*38*): K (bond stretching) = 1.341, H (bond angle bending) = 0.021, F (next nearest atom repulsion) = 0.214, Y (torsion) = 0.015, P (bond–bond interaction) = 0.175, and C (long range repulsion) = 0.070. For other values, see ref. (*19*); for valence force constants, see ref. (*38*). The bond–bond interaction constant P is unusually large, which has been rationalized by electron rearrangement during asymmetric stretching vibrations (*38*), as has also been found for S–S bonds (*39, 40*).

TABLE V

OBSERVED AND CALCULATED WAVE NUMBERS[a] OF THE 11 FUNDAMENTAL MODES OF CYCLOOCTASELENIUM, Se_8

	ν_1	ν_2	ν_3	ν_4	ν_5	ν_6	ν_7	ν_8	ν_9	ν_{10}	ν_{11}	Reference
Symmetry	a_1	a_1	b_1	b_2	e_1	e_1	e_2	e_2	e_2	e_3	e_3	
Observed	256	113	—	120	253	95	256	86	47	240	128	*3c,d,4b,37*
Calculated	255	111	231	120	255	97	255	88	46	240	127	*38*
Calculated	257	115	224	130	253	111	252	78	44	235	115	*19*

[a] In cm^{-1}.

The highly characteristic Se_8 Raman line at 113 cm^{-1} (totally symmetrical ring bending mode a_1) has occasionally been observed in the Raman spectrum of red amorphous Se(redn) (*3d, 37, 41*); this has been interpreted on the basis of either a certain Se_8 content of this material (*37, 41*) or of Se_8-like "molecular fragments" in a polymeric chain structure (*42*). However, the low-temperature Raman spectrum of red amorphous Se, recorded with the red line of a krypton laser (to avoid photodecomposition), does not exhibit this line (*14*). Instead, an almost continuous Raman scattering is observed for the region of the Se—Se—Se bending vibrations, indicating the presence of a large number of molecular species (e.g., rings) or of many different conformations of a long chain. The same holds for the Raman spectrum of freshly prepared red amorphous Se(vap), recorded at room temperature (*42*). The Se_8 signals in the earlier spectra are explained as photodecompositon of amorphous Se with formation of Se_8 in the laser beam (*14*).

The resonance Raman spectrum of a thin film of selenium exhibits 10 signals in the region 115–1400 cm^{-1}, which have been assigned to the fundamentals $\nu_2(a_1)$ and $\nu_{10}(e_3)$ of Se_8 and to their overtones and combination vibrations (*44*).

4. *Chemical Properties and Reactions*

Any external force, such as temperature or pressure, initiates the conversion of monoclinic selenium (Se_8) to the thermodynamically stable metallic modification. Both α-Se_8 and β-Se_8 are converted directly to the trigonal phase in the temperature range from 394 to 430 K, without being transformed into one another (*28, 45, 46*). Investigation of α-monoclinic Se_8 by DSC from 373 K up to the melting point of metallic selenium (494 K) has revealed an endothermic peak at 418 K and an exothermic peak at 430 K (heating rate 10 K/min), which have been interpreted by postulating melting of Se_8 followed by recrystallization to the metallic phase, respectively (*17*). Monoclinic selenium is thermodynamically unstable relative to metallic Se in the whole temperature range from 0 to 420 K (*47*). The conversion of Se_8 to Se_∞ depends on the quality of the crystals (*21, 48*) and gets complicated by premature melting of Se_8 if high heating rates are used (*21, 49, 50*). With single crystals of good quality investigated at 320 K/min, only one broad endothermic peak for the melting of monoclinic Se is observed [melting temperature, 429 K (*49*)], while at lower heating rates additional peaks for the exothermic conversion to solid metallic Se, followed by the endothermic melting of the latter, are found. The separation of the two melting peaks decreases with increasing heating rate

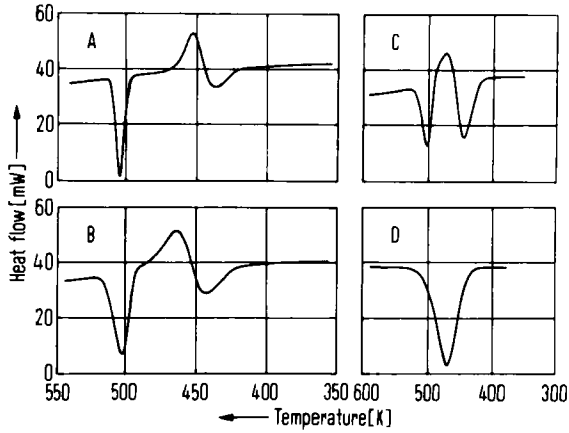

FIG. 6. DSC diagrams of single crystals of monoclinic α-Se_8 at different heating rates (sample mass, 4–5 mg) (*49*). Heating rates: A, 40; B, 80; C, 160; and D, 320 K/min.

and disappears at 320 K/min (*49*) (see Fig. 6). With a polycrystalline sample and a heating rate of 410 K/min, the melting point of monoclinic Se has been found to be 413 K (*50*), but extrapolation to zero heating rate indicates 428 K [Fig. 10 in ref. (*50*)].

Bombardment of monoclinic Se with fast electrons (*51*) or α particles (*52*) also results in conversion to the metallic phase. The mechanism of the conversion has been studied by X-ray diffraction, optical microscopy, and thermal analysis (*28, 46, 50*) and has been found to be topochemical. The formation of the crystal nuclei of the metallic phase is often related to larger lattice defects and occurs primarily at or near the crystal surface (*50*) and with an Arrhenius activation energy of 100 kJ/mol (*50*). The greater density of the metallic phase (see Table II) causes tensions that are responsible for the weakening of further Se—Se bonds. Ring opening of an Se_8 molecule is believed to be the rate-determining step of the metallic crystal growth though the mechanism discussed in Section III,B,3 may also be quite effective in transforming small rings into very large ones and vice versa:

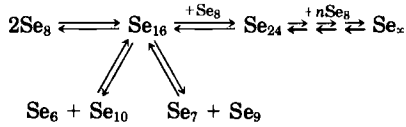

In the temperature range from 343 to 487 K, the metallic crystal growth has an activation energy of 113 kJ/mol (*50*) and 116.39 kJ/mol

(*53*), respectively. Comparison of the results of different authors makes it obvious that the process of conversion varies with temperature. To explain the effect of halogens, alkali metals, and amines, the following reactions have been proposed (*54*):

$$I_2 + (Se)_{ring} \longrightarrow ISe\text{—} \ldots \text{—}SeI + x(Se)_{ring} \longrightarrow I_2 + (Se)_{trig}$$

$$2Na + (Se)_{ring} \longrightarrow 2Na^+ + {}^-Se\text{—} \ldots \text{—}Se^- + x(Se)_{ring} \longrightarrow Na_2Se_y + (Se)_{trig}$$

$$R_3N + (Se)_{ring} \longrightarrow R_3N^+Se\text{—} \ldots \text{—}Se^- + x(Se)_{ring} \longrightarrow R_3N + (Se)_{trig}$$

Elemental selenium and elemental sulfur (any allotrope of either one) react on heating (melting) to give a large number of cyclic molecules Se_nS_m. While the eight-membered rings are much preferred, HPLC analysis has shown that both six- and seven-membered species are also formed. For a review of these cyclic selenium sufides, see ref. (*55*).

E. Other Ring Molecules

Investigations by mass spectrometry (see also Section III,C) have shown that molecules Se_n ($n = 2$–10) are the constituents of saturated selenium vapor (Knudsen cell) as well as of the vapor above freely subliming selenium (Langmuir cell), though the latter method yields a greater amount of the smaller molecules (*56*). Whereas Se_4, Se_8, Se_9, and Se_{10} are of minor significance, Se_5, Se_6, and Se_7 are the main components of selenium vapor in the temperature range from 473 to 650 K. At higher temperatures (up to 1400 K), the amount of the smaller noncyclic species, especially Se_2 and Se_3, increases rapidly (*9, 10, 57–60*).

Despite a large number of investigations, no agreement exists concerning the molecular composition of molten, quenched (glassy or vitreous), and red amorphous selenium. The usual, simplifying model of a dynamic equilibrium (*61*) of Se_8 rings and Se_n chains seems to explain the behavior of molten selenium qualitatively, but there are no reasons to exclude other small and medium sized rings, as have been detected in liquid sulfur (*1*). Several authors have pointed out that long chains as well as small and larger ring molecules may exist in glassy and in red amorphous selenium (*14, 17, 46*), the population of each component depending on the preparation procedure and the storage time and temperature.

F. Thermodynamic Properties of Selenium Allotropes

In connection with metallic selenium being a model compound for a homoatomic macromolecule, the heat capacity of selenium has been extensively studied. In a 1981 review (*63*) 23 investigations on the heat capacities of metallic, molten, amorphous, and monoclinic selenium have been critically evaluated, and a set of recommended data has been derived for the temperature range from 0 to 1000 K. The thermodynamic functions enthalpy, entropy, and Gibbs energy have been calculated. The heat capacity of metallic selenium is a smooth function of temperature from 0 K up to the melting point (494 K). The heat capacity of amorphous Se is also a smooth function of temperature from 0 to 270 K. An upward slope above 270 K can be associated with the glass transition. The heat capacity of monoclinic selenium below 100 K can be represented as an average of the heat capacities of metallic and amorphous Se. Above 100 K the heat capacities of monoclinic and metallic selenium are identical. Below 100 K the order of heat capacities is: amorphous > monoclinic > metallic. From 100 to 200 K the differences are minimal. Above 200 K the heat capacity of amorphous Se is higher than that of crystalline selenium. Setting the metallic selenium entropy at 0 K equal to zero, monoclinic selenium has, at 0 K, a residual entropy of about 1.7 J mol^{-1} K^{-1}, and the free enthalpy of the transition of monoclinic to metallic Se is negative; $\Delta G = -2.1$ kJ/mol(Se). At 0 K the residual entropy of amorphous (glassy) selenium is 3.63 J mol^{-1} K^{-1} and the free enthalpy of the transition of amorphous (glassy) to metallic selenium is equal to −3.8 kJ/mol. At 494.2 ± 0.1 K metallic selenium melts to an equilibrium melt with a heat of fusion of 6.20 kJ/mol and an entropy of fusion of 12.55 J mol^{-1} K^{-1}. Assuming that the equilibrium melt consists of 64% Se_8 rings and 36% long chains, the thermodynamic quantities for the monoclinic-to-melt transitions have been estimated as follows (*50*):

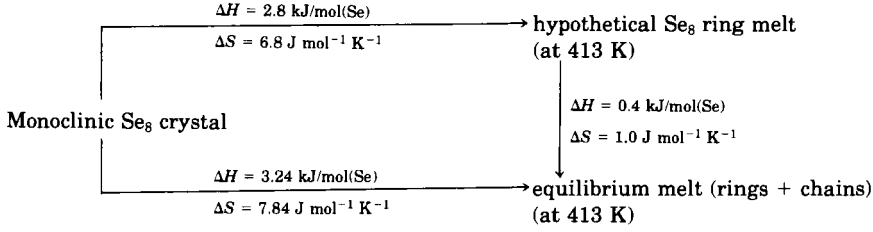

From these data it was concluded that, owing to the considerably higher enthalpy of fusion of metallic selenium, the slightly positive enthalpy for the reaction rings → chains in the melt is changed to a negative enthalpy of reaction for the ring-to-chain reaction in the crystalline state and makes the Se_8 rings metastable at all temperatures. The main reason for the higher stability of metallic selenium is its much higher packing density (see Table II) as a result of the fairly strong interchain attraction forces. According to Franz *et al.* (*49*) the enthalpy of fusion of α-monoclinic Se_8 amounts to 3.79 kJ/mol at 429 K.

The enthalpies of formation and atomization, the heat capacities, and the entropies of the selenium rings Se_n (n = 5–12), as derived from mass spectrometric measurements and statistical thermodynamics (*8–10, 12, 13, 57*), are given in Table VI.

The entropies, heat capacities, and thermodynamic functions of gaseous cyclooctaselenium have been calculated from spectroscopic and structural data for temperatures of up to 3000 K (*64*). Both the heat capacities and entropies of sulfur rings S_n (n = 6, 7, 8, 12) at a given temperature depend linearly on the ring size n (*65*). Therefore, it has been assumed that analogous relationships exist for the cyclic Se_n molecules, and the following equations have been derived from the data of Se_2 and Se_8 at 298 K (*64*):

$$C_p^\circ \text{ (J mol}^{-1}\text{ K}^{-1}\text{)} = 22.17n - 3.33$$

$$S_{298}^\circ \text{ (J mol}^{-1}\text{ K}^{-1}\text{)} = 49.6n + 135.4$$

The particular values are also listed in Table VI. It has further been found that at given temperatures $T_1 > T_2$ the function $H(T_1) - H(T_2)$ of S_n molecules depends on the number of atoms in the molecule. Provided an analogous relationship exists for Se_n molecules, corresponding equations can be derived from the data of Se_2 (*66*) and Se_8 (*64*), e.g.:

$$Se_n\text{: } H_{400} - H_{298} = 2.278n - 0.317 \text{ (kJ/mol)}$$

Equations of this type allow the functions $H(T_1) - H(T_2)$ to be calculated also for other Se_n (n = 5–12) molecules (*64*).

III. Homocyclic Selenium Cations

Cyclic selenium cations are known as monocations Se_n^+ observed in selenium vapor by mass spectrometry, and as dications Se_n^{2+} of which

TABLE VI

FORMATION ENTHALPIES ΔH_f°[a], ATOMIZATION ENTHALPIES ΔH_{at}°[a], ATOMIZATION ENTHALPIES REFERRED TO THE NUMBER OF ATOMS $\Delta H_{at}^{\circ}/n$[a], HEAT CAPACITIES C_p°[b], AND ENTROPIES S°[b] OF GASEOUS CYCLIC SELENIUM MOLECULES Se_n (n = 5–12)

	$\Delta H_{f,298}^{\circ}$		$\Delta H_{at,0}^{\circ}$	$\Delta H_{at,550}^{\circ}$	$\Delta H_{at}^{\circ}/n$		$C_{p,298}^{\circ}$	$\bar{C}_p$[c]	S_{298}°		S_{600}°
	10[d]	*8*	*9*	*57*	*9*	*57*	*64*	*12,13*	*64*	*10*	*9*
Se_5	148.7	170 ± 6	1042	946 ± 21	208	189 ± 4	107.5	100	383.4	405.9	458.5
Se_6	138.4	157 ± 6	1283	1183 ± 25	214	197 ± 4	129.7	124	433.0	444.7	523.9
Se_7	153.5	174 ± 6	1509	1390 ± 33	216	199 ± 5	151.9	147	482.6	507.9	592.9
Se_8	169.4	186 ± 6	1737	1624 ± 38	217	203 ± 5	174.0	170	532.2	565.6	655.6
Se_9	—	—	—	1796 ± 42	—	200 ± 5	196.2	—	581.8	—	—
Se_{10}	—	—	—	2010 ± 50	—	201 ± 5	218.4	—	631.4	—	—
Se_{11}	—	—	—	—	—	—	240.5	—	681.0	—	—
Se_{12}	—	—	—	—	—	—	262.7	—	730.6	—	—

[a] In kJ/mol.

[b] In J mol^{-1} K^{-1}.

[c] Average heat capacity in the temperature region 298–418 K.

[d] Reference.

those with $n = 4$, 8, or 10 have been isolated as salts with various anions. In general, the removal of electrons from neutral selenium molecules Se_n increases the total bond energy since the highest occupied molecular orbitals are always antibonding π orbitals. The ions formed therefore contain additional σ or π bonds as can be seen from the structures of Se_4^{2+}, Se_8^{2+}, and Se_{10}^{2+}. The structures of the monocations Se_n^+ are unknown.

A. Mass Spectra of Selenium Vapors

The mass spectra of evaporated elemental gray metallic selenium (Se_∞) have been investigated, using different techniques. Conventional heating to 102–187°C combined with ionization by electron impact (40 eV) leads to cations Se_n^+ with $n = 1$–10, Se_6^+ being the most abundant ion. Se_5^+, Se_6^+, Se_7^+, and Se_8^+ arise mainly from the corresponding cyclic molecules and not from fragmentation of larger molecular ions (*12*). For appearance potentials, see Table IV.

Heating of HgSe or of metallic selenium in a Knudsen cell (544–566 K) or surface evaporation of metallic or α-monoclinic Se, followed by electron impact ionization (75 eV), yields Se_n^+ ions with $n = 1$–8, Se_2^+ being the most abundant species (*8*). An investigation of the angular distribution of the ions Se_n^+ ($n = 1$–8) at different ionizing energies (8.5–75 eV) and 210°C (Knudsen cell temperature) provided special information concerning the fragmentation process within the ion source (*11*).

Evaporation of amorphous, metallic, or monoclinic Se by heating with a pulsed laser (10^7 W/cm^2, 800 μsec) also produces ions of type Se_n^+ ($n = 1$–9), Se_5^+ being the most abundant one. The analysis was carried out, using a time-of-flight mass spectrometer (*58, 67*).

Rather different spectra are obtained when the equilibrium vapor above metallic selenium (160°C) is ionized by a field ion source (2.5–8.0 kV), resulting in the ions Se_n^+ ($n = 2$ and 5–8); neither Se^+ nor Se_3^+ and Se_4^+ have been observed (these species usually result from fragmentation processes), but occasionally traces of Se_9^+ have been found. Using a Knudsen cell, Se_6^+ is the most abundant species, followed by Se_5^+ and Se_7^+, which all originate from the corresponding neutral, cyclic molecules (*56*). Field evaporation (20–100°C) of whiskers of selenium (prepared by field condensation of Se vapor) produces mainly Se_5^+, but small amounts of molecular ions with one, two, and four positive charges up to Se_{33} have been identified. However, these species may have chainlike structures (*56*).

TABLE VII

ELECTRONIC ABSORPTION AND DIFFUSE-REFLECTANCE SPECTRA OF THE Se_4^{2+} ION IN DIFFERENT ENVIRONMENTS (*70*)

Sample	Color	$\pi \rightarrow \pi^*$ (nm)	$\pi \rightarrow \pi^*$ or $\pi \rightarrow n^*$ (nm)
Se_4^{2+} in solution	Yellow	410	320
$Se_4(Sb_2F_4)(Sb_2F_5)(SbF_6)_5$	Golden yellow	413	382 (shoulder)
$Se_4(AsF_6)_2$	Yellow	440	385
$Se_4(AlCl_4)_2$	Yellow orange	488	430
$Se_4(HS_2O_7)_2$	Orange	524	428

B. DICATIONS Se_n^{2+} IN SOLIDS AND SOLUTIONS

1. *The* Se_4^{2+} *Ion*

The yellow, diamagnetic cation Se_4^{2+} was first detected by spectrophotometric and conductometric measurements on solutions of selenium in highly acidic and oxidizing solutions like $H_2S_2O_7$ (20°C), H_2SO_4 (95%, with SeO_2 or $K_2S_2O_8$ as oxidants), and HSO_3F (with $S_2O_6F_2$ as an oxidant) (*68*). Se_4^{2+} salts are prepared by reactions like:

$$4Se + S_2O_6F_2 \longrightarrow Se_4^{2+} + 2SO_3F^-$$

$$7Se + SeO_2 + 6H_2SO_4 \longrightarrow 2Se_4^{2+} + 6HSO_4^- + 2H_3O^+$$

$$4Se + 6H_2S_2O_7 \longrightarrow Se_4^{2+} + SO_2 + 2HS_3O_{10}^- + 5H_2SO_4$$

The formation of Se_4^{2+} proceeds via the green Se_8^{2+} as an intermediate (see below).

In solution, Se_4^{2+} exhibits an intense absorption at 410 nm and a very weak one at 330 nm (*68*). By dissolution of selenium in 65% oleum, in a mixture of HSO_3F with $S_2O_6F_2$, in liquid SO_3, or in excess liquid SbF_5, respectively, yellow to orange solids of compositions $Se_4(HS_2O_7)_2$, $Se_4(SO_3F)_2$, $Se_4(S_4O_{13})_2$, and $Se_4(Sb_2F_{11})_2$ can be prepared (*68*). AsF_5 reacts with Se in liquid SO_2 to give $Se_4(AsF_6)_2$ (*69*). The electronic transitions of these salts are shown in Table VII (*70*).

The shifts of the dipole-allowed $\pi \rightarrow \pi^*$ transition and of the weak band at lower wavelengths are caused by the varying polarizability of the anions and the fairly strong cation–anion interactions (*71*).

Mixtures of $SeCl_4$ and $AlCl_3$ show a melting point maximum of 203 ± 2°C at a mixing ratio of 2:1; the orange material is believed to consist of $Se_4(AlCl_4)_2$ on grounds of its IR spectrum (*72*).

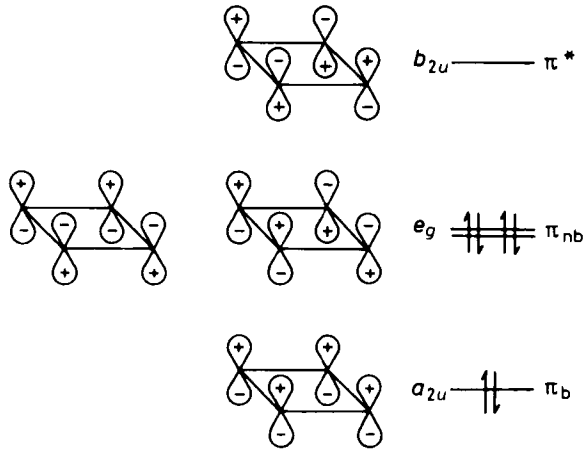

FIG. 7. Molecular orbitals of the π bond in Se_4^{2+} (π_b bonding, π_{nb} nonbonding, π^* antibonding).

Reaction of liquid SO_3 with metallic Se at ambient temperatures produces yellow solids indicated by analysis to be $Se_4S_nO_{3n+1}$ (n = 2, 3, 4) whose composition depends on the reaction time. UV spectra of solutions of these compounds in either H_2SO_4 or HSO_3F show the presence of Se_4^{2+} (*73*).

Crystals of $Se_4(HS_2O_7)_2$ have been examined by X-ray diffraction and were found to be monoclinic (space group $P2_1/c$) containing strictly square–planar Se_4^{2+} cations with an Se—Se internuclear distance of 228.3 pm (site symmetry C_i), significantly less than that of 234 pm found in the Se_8 molecule (see Table II). The shorter bond length has been explained by a delocalized π bond (*74, 75*). Each Se atom possesses six localized electron pairs. In addition, the four 3p orbitals perpendicular to the molecular plane form one bonding, two nonbonding, and one antibonding molecular orbitals, occupied by six electrons as shown in Fig. 7 (*76*). For a detailed MO theoretical study of Se_4^{2+}, see ref. (*77*).

X-ray structural studies were also performed on single crystals of $Se_4(Sb_2F_4)(Sb_2F_5)(SbF_6)_5$, prepared from Se and SbF_5 in liquid SO_2, and of $Se_4(AlCl_4)_2$ (*71, 78*). In both cases planar, centrosymmetrical cations with average bond distances of 226.0 and 228.6 pm, respectively, were found (valence angles, 90.0 ± 0.1°).

Extensive infrared, Raman, and resonance Raman (rR) spectroscopic investigations of solid and dissolved Se_4^{2+} salts led to the following

wave numbers of the four fundamental vibrations of the square–planar cation (*70, 76, 79*):

$$a_{1g} = 323,\ b_{1g} = 184,\ b_{2g} = 324\text{–}327,\ e_u = 302\ \text{cm}^{-1}$$

Eight combination vibrations and overtones, respectively, have been observed in the rR spectrum of Se_4^{2+} in 25% oleum, and these have been used to calculate the harmonic wave number $\omega_1 = 321.8 \pm 0.5\ \text{cm}^{-1}$ and the anharmonicity constants $x_{11} = -0.55$ and $x_{12} = -1.3\ \text{cm}^{-1}$ (*76*). Because of the high molecular symmetry, the spectroscopic data are insufficient to calculate accurate force constants, but when most of the interaction constants are neglected (i.e., set equal to zero) the following force constants for Se_4^{2+} can be deduced (in N/cm) (*70, 76*):

f_r (bond stretching) = 2.09

f_α (angle bending) = 0.20

f_{rr} (bond–bond interaction) = −0.02

f'_{rr} (nonneighboring bond interaction) = 0.36

Reactions. Salts containing the Se_4^{2+} ion are extremely hygroscopic, selenium being precipitated with excess water (*7*):

$$2Se_4^{2+} + 6H_2O \longrightarrow 7Se + SeO_2 + 4H_3O^+$$

Oxidation of Se_4^{2+} by peroxodisulfate, $S_2O_8^{2-}$, or peroxodisulfurylfluoride, $S_2O_6F_2$, leads to SeO_2, while reduction by either elemental selenium or hydrazine, N_2H_4, results in formation of the green Se_8^{2+} cation (*68*). Reaction of either $Se_4(AsF_6)_2$ or $Se_4(Sb_2F_{11})_2$ with S_4N_4 in liquid SO_2 produces blue-green crystals of $(Se_4S_2N_4)(AsF_6)_2$ and $(Se_4S_2N_4)(SbF_6)_2$, respectively, which contain the dimeric cation $Se_2SN_2^+$ shown in Fig. 8 (*69*).

2. *The* Se_8^{2+} *Ion*

The diamagnetic Se_8^{2+} ion was discovered by Gillespie *et al.* (*68*) by spectrophotometric and conductometric measurements on solutions of selenium in highly acidic and oxidizing solutions like H_2SO_4 [100% at 50–60°C, or 95% with $K_2S_2O_8$ or $Ce(SO_4)_2$ as an oxidant], $H_2S_2O_7$ (20°C), or HSO_3F (with SO_3 as an oxidant). In solution, Se_8^{2+} is dark green and is formed in reactions like the following:

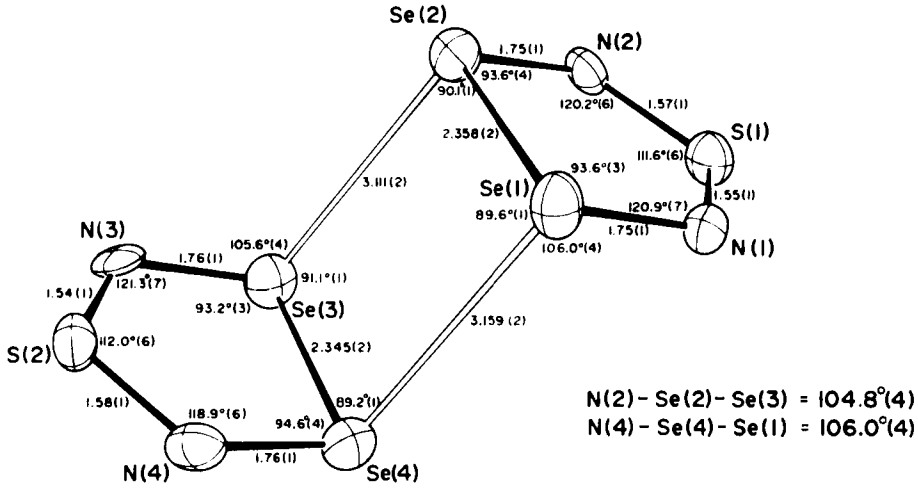

FIG. 8. Molecular structure of the cation in $(Se_4S_2N_4)(AsF_6)_2$ prepared from S_4N_4 and either Se_4^{2+} or Se_8^{2+} (*69*). Bond distances in angstroms. Numbers in parentheses are standard deviations.

$$8Se + 2H_2S_2O_7 \longrightarrow Se_8^{2+} + 2HSO_4^- + SO_2 + H_2SO_4$$

$$8Se + S_2O_8^{2-} \longrightarrow Se_8^{2+} + 2SO_4^{2-}$$

The green species has an intense absorption at 295 nm and weak ones at 470 and 685 nm (*68*).

Black prismatic crystals of $Se_8(AlCl_4)_2$ have been obtained from a stoichiometric mixture of $SeCl_4$, Se, and $AlCl_3$ after fusion at 250°C for 3 hr (*80*).

$$15Se + SeCl_4 + 4AlCl_3 \longrightarrow 2Se_8(AlCl_4)_2$$

The melting point of this compound was determined from the phase diagram of the Se–$SeCl_4$–$AlCl_3$ system to be 192°C (*72*).

An X-ray structural analysis of $Se_8(AlCl_4)_2$ revealed a bicyclic cation structure whose characteristic feature is an endo–exo conformation of the eight-membered ring. The molecular symmetry is approximately C_s (see Fig. 9).

The most striking detail of this structure is the transannular bond Se-3—Se-7 whose length of 284 pm is significantly less than the van der Waals distance (400 pm) and even less than the nonbonding contacts Se-2–Se-8 of 336 pm and Se-4–Se-6 of 330 pm. The other bond lengths vary between 229 and 236 pm and average to 231.8 pm (*80*).

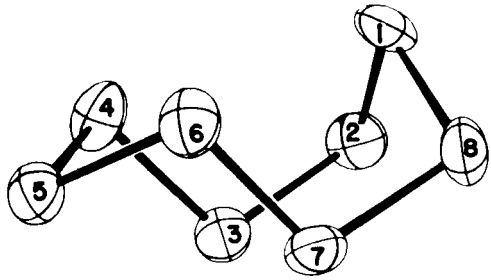

FIG. 9. Molecular conformation of the Se_8^{2+} ion in $Se_8(AlCl_4)_2$ (*80*). Bond distances (pm): 1–2, 229; 2–3, 233; 3–4, 230; 4–5, 233; 5–6, 231; 6–7, 231; 7–8, 236; 8–1, 231. Distance of Se-3 from Se-7 is 284 pm.

$Se_8(AlCl_4)_2$ can also be prepared according to the equation (*81*):

$$5Se_2Cl_2 + 4AlCl_3 \longrightarrow Se_8(AlCl_4)_2 + 2SeCl_3(AlCl_4)$$

The compounds $Se_8(AsF_6)_2$ and $Se_8(Sb_2F_{11})_2$ have been obtained as follows:

$$8Se + 3AsF_5 \xrightarrow[-23°C]{SO_2(l)} Se_8(AsF_6)_2 + AsF_3$$

$$8Se + 5SbF_5 \xrightarrow[0°C]{HF} Se_8(Sb_2F_{11})_2 + SbF_3$$

These green materials melt near 180°C and darken rapidly on exposure to moist air. When added to water they instantly decompose to red selenium and presumably SeO_2. Dissolution in H_2SO_4 (100%), oleum ($H_2SO_4 + SO_3$), or HSO_3F produces green solutions with the characteristic absorption maxima of Se_8^{2+} (see above). The formulas given above are based on analytical data and IR as well as NMR spectra (*82*). For a molecular orbital study of Se_8^{2+}, see ref. (*77*).

Reactions. $Se_8(AsF_6)_2$ reacts with S_4N_4 in liquid SO_2 at 20°C to give blue-green crystals of $(Se_4S_2N_4)(AsF_6)_2$, which contain the dimeric cyclic $Se_2SN_2^+$ cation shown in Fig. 8 (*69*). Oxidation of Se_8^{2+} in solution results in formation of the yellow Se_4^{2+} (see Section III,B,1), while reduction with elemental selenium produces the Se_{10}^{2+} cation (see Section III,B,3).

Solid $Se_8(AsF_6)_2$ reacts with C_2F_4 at room temperature to give AsF_3 and $(C_2F_5)_2Se_n$ with $n = 2$ or 3. $Se_8(Sb_2F_{11})_2$ yields similar products on reaction with C_2F_4 at 100°C. In SO_2 solution, $Se_8(AsF_6)_2$ and C_2F_4 yield mainly $(C_2F_5)_2Se_2$ and $F_5C_2SeSeCF_2COF$ (*83*).

3. *The* Se_{10}^{2+} *Ion*

Excess metallic selenium reacts with either AsF_5 or SbF_5 in SO_2 at 20–50°C to give the saltlike compounds $Se_{10}(AsF_6)_2$ and $Se_{10}(SbF_6)_2$, respectively, which have been obtained as deep-red crystals (brown when finely powdered) from the brownish-green solution. The reaction proceeds via Se_8^{2+}. An X-ray structural analysis of $Se_{10}(SbF_6)_2$ (space group $P2_1/n$, $Z = 8$) revealed a cation structure of the bicyclo[4.2.2.]decane type (*81*). The asymmetric unit contains two structurally similar molecules, one of which is shown in Fig. 10.

The Se—Se bond lengths alternate on moving away from the three-coordinated atoms: the six bonds adjacent to these three-coordinated atoms are the longest, having lengths of 241–246 pm; the bonds adjacent to these long bonds are shorter with lengths of 223–227 pm, and the unique central bond Se-13—Se-14 has an intermediate length of 236 pm (*81*). There are also some unusually short intramolecular Se ··· Se contacts between atoms that are not directly bonded, e.g., Se-18–Se-110 = 330 pm, Se-13–Se-19 = 339 pm, and Se-14–Se-17 = 349 pm indicating that Se_{10}^{2+} may be regarded as some kind of cluster molecule with partly delocalized valence electrons (*81*).

Considerable differences between the solution and solid-state colors and electronic absorption spectra have been observed that indicate that the stucture of the Se_{10}^{2+} cation is not retained in solution. $Se_{10}(MF_6)_2$ can be dissolved without decomposition in H_2SO_4 (95.5%), while in H_2SO_4 (100%) fairly rapid oxidation to Se_8^{2+} takes place (M = As or Sb) (*81*). $Se_{10}(AlCl_4)_2$ is obtained as a brown material by disproportionation of $Se_8(AlCl_4)_2$ on washing with large quantities of liquid SO_2 (*81*).

C. Other Dications

Spectrophotometric and potentiometric studies of the reduction of $SeCl_4$ by elemental selenium in eutectic $NaCl–AlCl_3$ melts at 150°C indicate that Se can exist in up to five different oxidation states, which have been interpreted in terms of the dications Se_n^{2+}, with $n = 2, 4, 8, 12$, or 16, but the exact nature and the structures of these species are unknown, and no pure compounds have been isolated from these mixtures (*84, 85*). Oxidation of $(C_2F_5)_2Se_2$ by either SbF_5 or $O_2(Sb_2F_{11})$ results in a wine-red cation of composition $(SeC_2F_5)_{2n}^{n+}$, where n is probably equal to 2. A homocyclic structure has been discussed for this species (*86*).

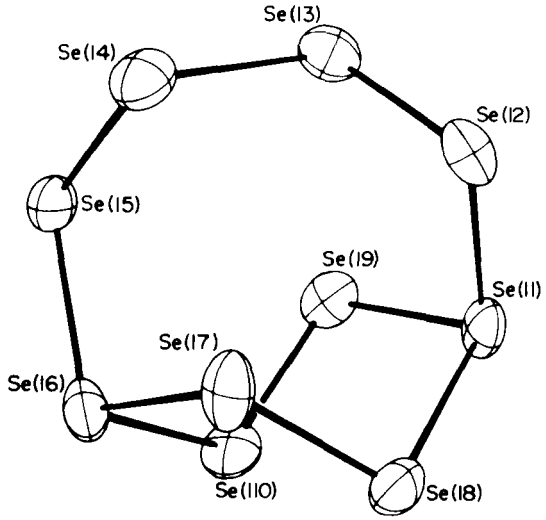

FIG. 10. Molecular conformation of the Se_{10}^{2+} ion in $Se_{10}(SbF_6)_2$ (*81*). Bond distances (pm): 11–12, 244; 12–13, 225; 13–14, 236; 14–15, 226; 15–16, 245; 16–17, 239; 17–18, 226; 18–11, 243; 11–19, 240; 19–110, 223; 110–16, 243.

IV. Selenium Iodide Cations, Se_nI^+

The first derivative of a selenium ring was prepared by Passmore *et al.* (*87*) according to the following equations:

$$32Se + 2I_2 + 9AsF_5 \longrightarrow 4(Se_6I)(AsF_6) + Se_8(AsF_6)_2 + 3AsF_3$$

$$12Se + I_2 + 3AsF_3 \longrightarrow 2(Se_6I)(AsF_6) + AsF_3$$

By X-ray crystallography it was shown that the monoclinic red-black crystals of Se_6IAsF_6 contain the homocyclic Se_6I^+ cation (symmetry C_s (*87*). The exocyclic iodine atom bridges neighboring Se_6 rings, the two SeI distances (273.6 pm) being equivalent and of bond order 0.5 (see Fig. 11).

The six-membered ring has a chairlike conformation and the Se—Se bond lengths vary between 229.2 and 237.0 pm. The longest bonds are those originating from the three-coordinated atoms, as has been observed for a number of related sulfur and selenium compounds, e.g., Se_{10}^{2+}, S_7I^+, or S_8O.

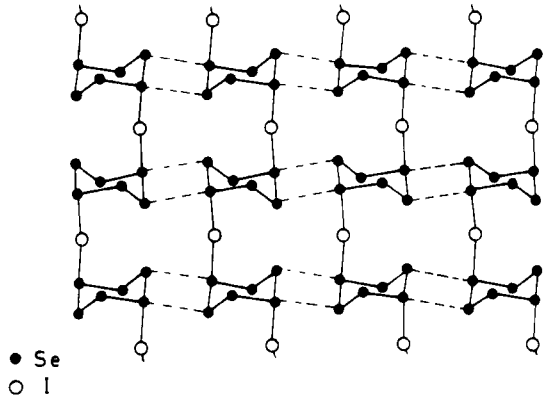

FIG. 11. Crystal structure of $(Se_6I)(AsF_6)$ (*87*).

Considerable intermolecular Se ··· Se interactions are a typical feature of the crystal structures of selenium rings, and this holds also for Se_6IAsF_6. Some of the contacts between neighboring rings are smaller than the sum of the van der Waals radii (400 pm), leading to a structure as shown in Fig. 11, in which polymeric strands of $[Se_6I^+]_n$ can be recognized. The dotted lines indicate stronger than van der Waals interactions (359.1 pm) (*87*).

No reactions of Se_6IAsF_6 are known.

V. Conclusions and Outlook

The structures and bond properties of the homocyclic species discussed in this article show that the selenium–selenium bond exhibits basically the same features as the well-investigated analogous sulfur–sulfur bond, which is known for its ability to adjust to a wide variety of bonding situations by large variations of the bond distances, bond angles, and dihedral angles (*36*). In the case of the Se—Se bonds, the fewer number of examples does not yet allow a systematic analysis, but contrary to what has been assumed in the past (when the importance of partial as well as double bonds between second- and third-row elements has been underestimated or even denied), the presently known examples show that the Se—Se bond order in homocyclic molecules can vary over a wide range, as reflected by variation of the bond distances between the 284 pm in Se_8^{2+} and 223 pm in Se_{10}^{2+}. These values should be compared with the bond length in the strain-free ring of Se_8 (234 pm) as a measure of the single-bond length and with the van der

Waals distance of 400 pm as an upper limit. A stable homocyclic compound with a selenium–selenium double bond is not known.

It can be expected that the relationships between (1) bond length and dihedral angle, (2) bond length and stretching force constant, and (3) bond length and the length of the neighboring bonds, which have been established empirically for homocyclic sulfur molecules (*1, 36*), will also be found in the case of selenium rings as soon as sufficiently different structures are known.

One of the major differences between two-coordinated sulfur and selenium is the tendency of the latter to increase its coordination number, as can be seen from the fairly strong intermolecular interactions between selenium rings in the various crystal structures. The shortest intermolecular distance observed (335 pm in γ-Se_8) is 65 pm shorter than the van der Waals distance (400 pm) but still 101 pm longer than the single bond distance defined above. In the case of sulfur rings the shortest observed intermolecular contact (323 pm in S_{10} (*88*) is 37 pm shorter than the van der Waals distance (360 pm) but 101 pm longer than the single bond in S_8.

Many of the above-mentioned compounds have been first prepared or properly characterized after 1968. It therefore can be expected that new species of similar types will be synthesized in the near future. Their investigation by modern analytical techniques will finally help to elucidate the molecular structure of more complex systems such as amorphous, glassy, and liquid elemental selenium. In this context the already better understood homocyclic sulfur compounds and, in particular, the mixed species, the heterocyclic selenium sulfides (*55*), can serve as models to study the structural and chemical behavior of the selenium–selenium bond.

REFERENCES

1. Steudel, R., *Top. Curr. Chem.* **101,** 149 (1982).
2. Laur, P. H., *in* "Sulfur in Organic and Inorganic Chemistry" (A. Senning, ed.), Vol. 3, p. 91. Dekker, New York, 1972.
3. Cooper, W. Ch., ed., "The Physics of Selenium and Tellurium." Pergamon, London, 1969. (*a*) Abdullayev, G. B., Asadov, Y. G., and Mamedov, K. P., p. 179. (*b*) Izima, S., Taynai, J., and Nicolet, M. A., p. 199. (*c*) Lucovsky, G., p. 255. (*d*) Mooradian, A., and Wright, G. B., p. 269.
4. Zingaro, R. A., and Cooper, W. Ch., eds., "Selenium." Van Nostrand-Reinhold, Princeton, New Jersey, 1974. (*a*) Cooper, W. Ch., and Westbury, R. A., p. 87. (*b*) Zallen, R., and Lucovsky, G., p. 148.
5. Gmelin Handbuch der anorganischen Chemie, "Selenium," Vol. A2, p. 179. Springer-Verlag, Berlin and New York, 1980.

6. Gillespie, R. J., and Passmore, J., *Adv. Inorg. Chem. Radiochem.* **17,** 51 (1975).
7. Gillespie, R. J., *Chem. Soc. Rev.* **8,** 315 (1979).
8. Berkowitz, J., and Chupka, W. A., *J. Chem. Phys.* **45,** 4289 (1966); *J. Chem. Phys.* **48,** 5743 (1968).
9. Keller, H., Rickert, H., Detry, D., Drowart, J., and Goldfinger, P., *Z. Phys. Chem. (Frankfurt)* **75,** 273 (1971).
10. Rau, H., *J. Chem. Thermodyn.* **6,** 525 (1974).
11. Grimley, R. T., Grindstaff, Q. G., DeMercurio, T. A., and Forsman, J. A., *J. Phys. Chem.* **86,** 976 (1982).
12. Fujisaki, H., Westmore, J. B., and Tickner, A. W., *Can. J. Chem.* **44,** 3063 (1966).
13. Westmore, J. B., Fujisaki, H., and Tickner, A. W., *Adv. Chem. Ser.* **72,** 231 (1968).
14. Steudel, R., and Strauss, E.-M., *Z. Naturforsch.* **36b,** 1085 (1981).
15. Steudel, R., and Strauss, E.-M., unpublished results.
16. Miyamoto, Y., *Jpn. J. Appl. Phys.* **16,** 2257 (1977).
17. Miyamoto, Y., *Jpn. J. Appl. Phys.* **19,** 1813 (1980).
18. Nagata, K., Ishibashi, K., and Miyamoto, Y., *Jpn. J. Appl. Phys.* **19,** 1569 (1980).
19. Nagata, K., Ishibashi, K., and Miyamoto, Y., *Jpn. J. Appl. Phys.* **20,** 463 (1981).
20. Mäusle, H.-J., and Steudel, R., *Z. Anorg. Allg. Chem.* **463,** 27 (1980).
21. Gobrecht, H., Willers, G., and Wobig, D., *Z. Phys. Chem. (Frankfurt)* **77,** 197 (1972); *J. Phys. Chem. Solids* **31,** 2145 (1970).
22. Gattow, G., and Heinrich, G., *Z. Anorg. Allg. Chem.* **331,** 275 (1964).
23. Barzdain, P. P., and Alekseev, N. V., *Zh. Struct. Khim.* **9,** 520 (1968). *J. Struct. Chem.* USSR **9,** 442 (1968).
24. Steudel, R., and Schuster, F., *J. Mol. Struct.* **44,** 143 (1978).
25. Nagata, K., Tashiro, H., and Miyamoto, Y., *Jpn. J. Appl. Phys.* **20,** 2265 (1981).
26. Keezer, R. C., and Geils, R. H., unpublished results cited in ref. *43.*
27. Burbank, R. D., *Acta Crystallogr.* **4,** 140 (1951).
28. Marsh, R. E., Pauling, L., and McCullough, J. D., *Acta Crystallogr.* **6,** 71 (1953).
29. Foss, O., and Janickis, V., *J. Chem. Soc. Chem. Commun.* 834 (1977); *J. Chem. Soc. Dalton Trans.,* 624 (1980).
30. Grunwald, H. P., *Mater. Res. Bull.* **7,** 1093 (1972).
31. Cherin, P., and Unger, P., *Acta Crystallogr.* **B28,** 313 (1972).
32. Cherin, P., and Unger, P., *Inorg. Chem.* **8,** 1589 (1967).
33. Donohue, J., "The Structures of the Elements." Wiley, New York, 1974.
34. Briegleb, G., *Z. Phys. Chem. A* **144,** 321, 340 (1929).
35. Moody, J. W., and Himes, R. C., *Mater. Res. Bull.* **2,** 523 (1967).
36. Steudel, R., *Angew. Chem.* **87,** 683 (1975); *Angew. Chem. Int. Ed.* **14,** 655 (1975).
37. Lucovsky, G., Mooradian, A., Taylor, W., Wright, G. B., and Keezer, R. C., *Solid State Commun.* **5,** 113 (1967).
38. Steudel, R., *Z. Naturforsch.* **30a,** 1481 (1975).
39. Steudel, R., *Z. Naturforsch.* **30b,** 281 (1975).
40. Steudel, R., *Spectrochim. Acta* **31A,** 1065 (1975).
41. Gorman, M., and Solin, S. A., *Solid State Commun.* **18,** 1401 (1976).
42. Lucovsky, G., *in* "The Physics of Selenium and Tellurium," (E. Gerlach and P. Grosse, (eds.), p. 178. Springer-Verlag, Berlin and New York, 1979.
43. Zirke, J., Dissertation, Techn. Univ. Berlin, 1976.
44. Ohta, N., Scheuerman, W., and Nakamoto, K., *Solid State Commun.* **27,** 1325 (1978).
45. Laitinen, R., and Niinistö, L., *J. Therm. Anal.* **13,** 99 (1978).
46. Asadov, Y. G., *Kristallografiya* **14,** 356 (1969); *Sov. Phys. Crystallogr.* **14,** 292 (1969); *Dokl. Akad. Nauk SSSR* **173,** 570 (1967); *Sov. Phys. Dokl.* **12,** 199 (1967).
47. Shu, H.-C., Gaur, U., and Wunderlich, B., *Thermochim. Acta* **34,** 63 (1979).

48. Meissner, M., Tausend, A., and Wobig, D., *Phys. Status Solidi* **A49,** 59 (1978).
49. Franz, P., Gobrecht, H., Scheiba, M., Wobig, D., and Kunze, W., *Z. Phys. Chem. (Frankfurt)* **111,** 163 (1978).
50. Murphy, K. E., Altmann, M. B., and Wunderlich, B., *J. Appl. Phys.* **48,** 4122 (1977).
51. Belin, E., Bonnelle, C., and Delafosse, D., *J. Appl. Crystallogr.* **4,** 383 (1971).
52. Stech, B., *Z. Naturforsch.* **7a,** 175 (1952).
53. Asadov, Y. G., *Fiz. Svoistva Selena Selenovykh Prib.* **21,** after *Chem. Abstr.* 82 (1974); **78,** 844 (1975).
54. Krebs, H., *Z. Anorg. Allg. Chem.* **265,** 156 (1951); *Angew. Chem.* **65,** 293 (1953).
55. Steudel, R., and Laitinen, R., *Top. Curr. Chem.* **103,** 177 (1982).
56. Saure, H., and Block, J., *Int. J. Mass Spectrom. Ion Phys.* **7,** 145 and 175 (1971).
57. Hoareau, A., Reymond, J.-M., Cabaud, B., and Uzan, R., *J. Phys. (Paris)* **36,** 737 (1975).
58. Knox, B. E., *Mater. Res. Bull.* **3,** 329 (1968); *Adv. Mass. Spectrom.* 4, 491 (1968).
59. Streets, D. G., and Berkowitz, J., *J. Electron. Spectrosc. Relat. Phenom.* **9,** 268 (1976).
60. Rau, H., *Ber. Bunsenges. Phys. Chem.* **71,** 711 (1967).
61. Eisenberg, A., and Tobolsky, A. V., *J. Polymer Sci.* **46,** 19 (1960).
62. Gobrecht, H., Willers, G., Wobig, D., and Zirke, J., *Z. Naturforsch.* **27a,** 1246 (1972).
63. Gaur, U., Shu, H.-C., Mehta, A., and Wunderlich, B., *J. Phys. Chem. Ref. Data* **10,** 89 (1981).
64. Steudel, R., *Z. Naturforsch.* **36a,** 408 (1981).
65. Steudel, R., and Mäusle, H.-J., *Z. Naturforsch.* **33a,** 951 (1978).
66. Mills, K. C., "Thermodynamic Data for Inorganic Sulfides, Selenides and Tellurides," p. 86. Butterworths, London, 1974.
67. Ban, V. S., and Knox, B. E., *Int. J. Mass Spectrom. Ion Phys.* **3,** 131 (1969).
68. Barr, J., Gillespie, R. J., Kapoor, R., and Malhotra, K. C., *Can. J. Chem.* **46,** 149 and 3607 (1968).
69. Gillespie, R. J., Kent, J. P., and Sawyer, J. F., *Inorg. Chem.* **20,** 4053 (1981).
70. Burns, R. C., and Gillespie, R. J., *Inorg, Chem.* **21,** 3877 (1982).
71. Cardinal, G., Gillespie, R. J., Sawyer, J. F., and Vekris, J. E., *J. Chem. Soc. Dalton Trans.* 765 (1982).
72. Prince, D. J., Corbett, J. D., and Garbisch, B., *Inorg. Chem.* **9,** 2731 (1970).
73. Paul, R. C., Arora, C. L., Virmani, R. N., and Malhotra, K. C., *Indian J. Chem.* **9,** 368 (1971).
74. Brown, I. D., Crump, D. B., Gillespie, R. J., and Santry, D. P., *J. Chem. Soc. Chem. Commun.* 583 (1968).
75. Brown, I. D., Crump, D. B., and Gillespie, R. J., *Inorg. Chem.* **10,** 2319 (1971).
76. Clark, R. J. H., Dines, T. J., and Ferris, L. T. H., *J. Chem. Soc. Dalton Trans.* 2237 (1982).
77. Tanaka, K., Yamabe, T., Terama-e, H., and Fukui, K., *Inorg. Chem.* **18,** 3591 (1979); *Nouv. J. Chim.* **3,** 379 (1979).
78. Brown, I. D., Crump, D. B., and Gillespie, R. J., *Inorg. Chem.* **10,** 2319 (1971).
79. Gillespie, R. J., and Pez, G. P., *Inorg. Chem.* **8,** 1229 (1969).
80. McMullan, R. K., Prince, D. J., and Corbett, J. D., *Inorg Chem.* **8,** 1749 (1971); *J. Chem. Soc. Chem. Commun.* 1438 (1969).
81. Burns, R. C., Chan, W.-L., Gillespie, R. J., Luk, W.-C., Sawyer, J. F., and Slim, D. R., *Inorg. Chem.* **19,** 1432 (1980).
82. Gillespie, R. J., and Ummat, P. K., *Can. J. Chem.* **48,** 1239 (1970).
83. Desjardins, C. D., and Passmore, J., *J. Chem. Soc. Dalton Trans.* 2314 (1973).

84. Fehrman, R., Bjerrum, N. J., and Andreasen, H. A., *Inorg. Chem.* **14,** 2259 (1975).
85. Fehrmann, R., and Bjerrum, N. J., *Inorg. Chem.* **16,** 2089 (1977).
86. Passmore, J., Richardson, E. K., and Taylor, P., *J. Chem. Soc. Dalton Trans.* 1006 (1976).
87. Shanta Nandana, W. A., Passmore, J., and White, P. S., *J. Chem. Soc. Chem. Commun.* 526 (1983).
88. Reinhardt, R., Steudel, R., and Schuster, F., *Angew. Chem.* **90,** 55 (1978); *Angew. Chem. Int. Ed.* **17,** 57 (1978); Steudel, R., Steidel, J., and Reinhardt, R., *Z. Naturforsch.* **38b,** 1548 (1983).